

Cosmological bounds on a possible electron-to-proton mass ratio variation and constraints in the lepton specific 2HDM

R. G. Albuquerque^{1,*}, R. F. L. Holanda^{2,3,†}, I. E. T. R. Mendonça^{2,5,‡} and P. S. Rodrigues da Silva^{1,§}

¹*Departamento de Física, Universidade Federal da Paraíba,
Caixa Postal 5008, 58051-970, João Pessoa, PB, Brasil*

²*Departamento de Física, Universidade Federal do Rio Grande do Norte,
Natal - Rio Grande do Norte, 59072-970, Brasil*

³*Departamento de Física, Universidade Federal de Campina Grande, 58429-900, Campina Grande - PB, Brasil and*

⁵*Biofy.tech IA Department, 38407-180, Uberlândia-MG Brazil*

In this work, we test a possible redshift variation of the electron-to-proton mass ratio, $\mu = m_e/m_p$, directly from galaxy cluster gas mass fraction measurements and type Ia supernovae observations. Our result reveals no variation of μ within 1σ . From the point of view of Particle Physics, we can use the precision on these results to constrain the parameter space of models beyond the Standard Model of electroweak interactions. We exemplify this by focusing on a specific Two-Higgs doublet model (2HDM), where the second scalar doublet couples exclusively to leptons. An important parameter in the model concerns the ratio between its vacuum expectation values, defined by $\tan\beta \equiv v_2/v_1$. In our approach, we can constrain the inverse parameter ($\cot\beta$) to an optimal value, $(\cot\beta) = (2.003 \pm 0.081) \cdot 10^{-3}$, with the highest vacuum expectation value for 2HDM, v_2 , estimated at around 240.57 ± 2.93 GeV. Also, by taking into account the discrepancy in the anomalous magnetic moment of the muon found between theory and experiment, we can reduce the validity region for this model and establish bounds on the scalar masses, in light of our findings from galaxy cluster data for μ . This study contributes valuable insights to the understanding of the interface between Particle Physics and Astrophysics, establishing a new interrelationship between data on the large-scale structure of the Universe and subatomic Physics.

PACS numbers: 98.62.Ra, 98.65.-r, 98.80.-k, 12.60.Fr, 14.80.Ec

I. INTRODUCTION

Fundamental physical theories rely on certain parameters known as fundamental constants, such as the fine-structure constant, gauge couplings, and Yukawa couplings. Their values cannot be predicted from existing knowledge and must be determined through experimentation. These constants are traditionally assumed to be mathematical constructs that are unchanging across both time and space, as posited by the simplest and most successful physical theories. Dirac [1] was among the first to question whether these constants are merely mathematical constructs or if they hold deeper significance within a broader cosmological framework. Current laboratory experiments have ruled out significant variations in these constants on laboratory [2], geological [3, 4], and solar system time scales [5]. Astrophysical methods, particularly the spectroscopy of quasar absorption lines, which involves measuring transition wavelengths at high redshifts over vast time intervals, prove a much broader time span [6–9].

In recent years, observational tests investigating possible variations in fundamental constants have proliferated in the literature (see [10–13] for a review). In this context, two dimensionless constants, the fine-structure constant ($\alpha \equiv e^2/4\pi\epsilon_0\hbar c$) and the electron-to-proton mass ratio ($\mu \equiv m_e/m_p$), are of particular importance. These constants are not only interrelated, but their potential variation is also connected to new physics, including models of extended gravity [14–16], string theory [17, 18], and more recently dark matter models [19, 20]. Thus, constraining the temporal and spatial variations of these parameters could have profound implications for both cosmology and fundamental physics. The use of large-scale structure physics, particularly the physics of galaxy clusters, to constrain variations in α is not new [21]; however, it has become an area of intense investigation in recent years [22–27]. In contrast, no studies have yet addressed the issue of μ variation using galaxy clusters, a path that we aim to explore in this work.

Concerning small-scale physics, the Standard Model of Electroweak Interactions¹ (SM) has been thoroughly con-

*Electronic address: rennan.gomes@ufabc.edu.br

†Electronic address: holandarfl@fisica.ufrn.br

‡Electronic address: isaacmendonca@biofy.tech

§Electronic address: psilva@fisica.ufpb.br

¹ We will neglect the strong interaction sector of the Standard Model of Particle Physics in this work, the $SU(3)_C$ part of the gauge

firmed over the past decades through several collider data measurements, culminating in the discovery of the last important ingredient predicted by the model, the Higgs boson, at the Large Hadron Collider (LHC)[28–30]. This was a significant step in definitively establishing the SM as a fiducial paradigm for describing the visible matter content in the Universe and its interactions in a detailed and precise way. However, it is not the most complete theory we can imagine. This is because there are several unresolved issues, such as the evidence for Cold Dark Matter[31], the mass and oscillation of neutrinos [32, 33], and the experimental deviation from the theoretical prediction of the muon anomalous magnetic moment [34, 35], among others, that cannot be addressed by the model without extending its matter or interaction content (gauge group). In this sense, several models have been proposed in the literature to go beyond the SM. A particular class of interest for phenomenologists is the so-called Two-Higgs Doublet Model (2HDM)[36, 37], especially since the scalar sector of the SM is under intense scrutiny. An extra scalar doublet represents the simplest component of supersymmetric theories² that can be studied theoretically without necessarily addressing the specific details of the intricate spectrum of such theories. In addition, 2HDM can introduce sources of CP violation in the scalar sector [41], allowing baryogenesis in this class of models [42, 43]. The extra neutral scalar can also offer a richer vacuum structure that could lead to a first-order phase transition [44–47], another requirement for baryogenesis. Finally, it is well known that additional scalar doublets do not alter the SM prediction for the observable ρ -parameter³.

Our main goal in this work is to constrain a possible redshift variation in the electron-to-proton mass ratio, $\mu \equiv m_e/m_p$, using observational data, specifically galaxy cluster gas mass fraction measurements and Type Ia supernova luminosity distances, and to impose limits on particle physics models beyond the Standard Model (SM). We focus on a specific version of the 2HDM, where leptons and quarks interact with different scalar doublets. Since the constraint on μ from galaxy clusters is directly related to the ratio between the vacuum expectation values (vev) of the model⁴, we can use these constraints on μ to derive bounds on the parameters of the 2HDM. To impose tighter limits on the parameter space, including the scalar masses of the model, we also compute the anomalous magnetic moment of the muon, restricting the analysis to the region of parameters that can resolve the 4.2σ discrepancy between experiment and theory. This discrepancy currently represents one of the most promising indications of physics beyond the SM [48].

The manuscript is organized as follows: we first present the methodology by which we derive the relation between the electron-to-proton mass ratio and the galaxy cluster gas mass fraction in Section II. Then, in Section III, we briefly explain the cosmological data sample used in our analysis. We describe, in Section IV, the theoretical structure of the 2HDM that we base our investigation. In Section V we describe the details of our analysis and the results we get for the μ variation. After that, in Section VI, we present constraints on $\tan\beta$, as well as the masses of the heavier Higgs in the 2HDM, including the computation of the muon anomalous magnetic moment contribution to solve the theoretical-experimental discrepancy. Finally, we draw our conclusions and share some perspectives in Section VII.

II. ELECTRON-TO-PROTON MASS RATIO AND GALAXY CLUSTER GAS MASS FRACTION

Galaxy clusters are the largest virialized structures in the universe [49]. They are predominantly composed of dark matter and hot intergalactic gas, referred to as the Intra-Cluster Medium (ICM). The ICM, in a plasma state, emits a continuous X-ray spectrum primarily dominated by thermal bremsstrahlung, with typical temperatures ranging between 2 and 10 keV [50]. The ratio of ICM mass to total cluster mass, that is, the gas mass fraction f_{gas} , is of particular significance in cosmology, as it allows constraints on cosmological parameters [51–53]. Moreover, it enables various tests on the fundamental physics, including, for instance, the exploration of fundamental constant variations [24, 54] and violations of Einstein’s equivalence principle [55–57]. Consider the gas mass, M_{gas} , within a radius R ,

symmetry group, as it is not important for the entire analysis we deal with.

² Supersymmetric theories (for a review, see Ref. [38–40] and references therein) have been extensively investigated for decades, as they are a fundamental component for the mathematical consistency of string theory. However, no evidence of supersymmetry has been observed in accelerators to date.

³ The ρ -parameter is defined (at tree level) as $\rho_{tree} = \frac{M_W^2}{M_Z^2 \cos^2 \theta_W}$, where M_W and M_Z are the masses of the W and Z weak gauge bosons, respectively, and θ_W is the weak mixing angle. Its theoretical value in the SM is $\rho_{tree} = 1$.

⁴ As we will see, in our approach we restrict the variation in the electron-to-proton mass ratio to the electron mass only. This restriction allows us to infer that the ratio of vev in the 2HDM, namely $\tan\beta$, is the parameter constrained by the μ variation.

obtained through X-ray spectrum measurements [50, 58]:

$$M_{gas}(< R) = \left(\frac{3\pi\hbar m_e c^2}{2(1+X)e^6} \right)^{1/2} \left(\frac{3m_e c^2}{2\pi k_B T_e} \right)^{1/4} M_H \times \frac{1}{[\bar{g}_B(T_e)]^{1/2}} r_c^{3/2} \left[\frac{I_M(R/r_c, \beta)}{I_L^{1/2}(R/r_c, \beta)} \right] [L_X(< R)]^{1/2}. \quad (1)$$

Here, X is the fraction of Hydrogen mass in the gas, m_e and M_H are the masses of the electron and Hydrogen⁵, respectively. T_e is the gas temperature, \bar{g}_B is the Gaunt factor, a multiplicative correction to take quantum effects into consideration for the calculations of absorption or emission of radiation [59], and r_c is the core radius. I_M and I_L are defined as:

$$I_M(y, \beta) \equiv \int_0^y (1+x^2)^{-3\beta/2} x^2 dx,$$

$$I_L(y, \beta) \equiv \int_0^y (1+x^2)^{-3\beta} x^2 dx,$$

obtained using a spherical β model, and the bolometric luminosity $L_X(< R)$ is given by:

$$L_X(< R) = 4\pi [D_L(z, \Omega_0, H_0)]^2 f_X(< \theta),$$

where $f_X(< \theta)$ is the total bolometric flux within the outer angular radius θ [60]. D_L is the luminosity distance, which depends on the redshift, z , the cosmological density parameter, Ω_0 , and the Hubble parameter, H_0 . The total cluster's mass, M_{tot} , obtained by using the Euler equation for a fluid in hydrostatic equilibrium, with the additional assumption of isothermality [61], is given by:

$$M_{tot}(< R) = - \frac{k_B T_e R}{G x_H M_H} \frac{d \ln n_e(r)}{d \ln r} \Big|_{r=R}. \quad (2)$$

Here, x_H is the molar fraction of hydrogen in the gas, G is Newton's gravitational constant, and n_e is the electron gas density. Thus, from Eq. (1), we observe that $M_{gas} \propto M_H$, and from Eq. (2), $M_{tot} \propto 1/M_H$. Consequently, we can conclude that the gas mass fraction, f_{gas} within the intra-cluster medium, which is the ratio between Eq. (1) and Eq. (2),

$$f_{gas} \propto M_H^2, \quad (3)$$

and since $M_H = m_e + m_p$ ⁶, then

$$f_{gas} \propto (1 + \mu)^2 m_p^2, \quad (4)$$

which, as we can see, explicitly depends on μ , the ratio of electron to proton masses.

On the other hand, the expected constancy of f_{gas} within massive, hot and relaxed galaxy clusters with redshifts in the interval of interest has been used to constrain cosmological parameters via the following equation [51–53]:

$$f_{gas}^{th}(z) = \gamma(z) K_0 A(z) \frac{\Omega_b}{\Omega_m} \left[\frac{D_L^{ref}}{D_L} \right]^{3/2}. \quad (5)$$

In Eq. (5), D_L^{ref} represents the luminosity distance of the cluster calculated using a fiducial concordance model (the flat Λ CDM model with $H_0 = 70$ and $\Omega_m = 0.3$), while D_L is the actual luminosity distance of the cluster. The term $\gamma(z)$ is the baryon depletion factor, expressed as

$$\gamma(z) = \gamma_0 (1 + \gamma_1 z) \left(\frac{M_{2500}}{3 \times 10^{14} M_\odot} \right)^\alpha,$$

⁵ We designate the mass of Hydrogen with a capital M to avoid confusion with the mass of the heavy Higgs to be defined later in the article.

⁶ Here we neglect the binding energy of the hydrogen atom, since it is of the order of $\sim 10^{-4}$ of the electron mass.

where $\alpha = 0.025 \pm 0.033$, $\gamma_0 = 0.79 \pm 0.11$ and $\gamma_1 = 0.07$. The last two values were obtained from hydrodynamical simulations in Refs. [62–64]. The parameters Ω_b and Ω_m represent the baryonic and matter density parameters, respectively. The term $K_0 = 0.96 \pm 0.12$ refers to the mass calibration factor, which was determined using 13 clusters from the sample, incorporating weak gravitational lensing measurements from the Weighting the Giants project [65]. The $A(z)$ term represents the angular correction factor, defined as

$$A(z) = \frac{H(z) d(z)}{[H(z) d(z)]^{\text{ref}}},$$

where $H(z) = \sqrt{\Omega_m(1+z)^3 + (1-\Omega_m)}$, and $d(z)$ is the comoving distance to the cluster (here $\Omega_m = 0.315 \pm 0.007$ and $H_0 = 67.36 \pm 0.54$ km/s/Mpc since we have considered the flat Λ CDM model [66]).

Thus, considering a possible variation of μ with redshift, we modify Eq. (5) accordingly, arriving at the expression:

$$f_{gas}^{obs} = (1 + \mu(z))^2 \gamma(z) K_0 A(z) \frac{\Omega_b}{\Omega_m} \left[\frac{D_L^*}{D_L} \right]^{3/2}. \quad (6)$$

Finally, if the luminosity distance is known for each galaxy cluster, $\mu(z)$ can be inferred through the deviation from zero of $(1 + \mu)^2$ with respect to the ratio

$$\frac{f_{gas}^{obs}}{f_{gas}^{th}},$$

where f_{gas}^{obs} is the observed gas mass fraction and f_{gas}^{th} is the theoretical gas mass fraction.

$$(1 + \mu)^2 - \frac{f_{gas}^{obs}}{f_{gas}^{th}} = 0, \quad (7)$$

where f_{gas}^{obs} is the gas mass fraction dataset⁷ presented in Section III and f_{gas}^{th} comes from Eq. (5). This will provide 40 values of μ (see Table II), which will be used to obtain the expected variation in the range of redshifts presented, i.e., $\Delta\mu$. Also, those 40 points will be used to reconstruct the function $\mu(z)$ via Gaussian process regression, as we describe next. We have used $\Omega_b/\Omega_m = 0.157 \pm 0.002$ as given by Planck’s results [66].

III. COSMOLOGICAL DATA

A. Gas Mass Fraction

We utilize the recent sample of 40 f_{gas} measurements spanning the redshift range $0.018 \leq z \leq 1.160$, compiled in Ref. [53]. This dataset comprises 40 massive, hot, and morphologically relaxed galaxy clusters observed by the Chandra telescope (see Fig. 1). The selection of relaxed systems aims to minimize systematic biases in the hydrostatic masses. The gas mass fraction is computed within the spherical shell defined by $0.25 \leq r/r_{2500} \leq 0.8$ rather than integrated over all radii. Further details about the data can be found in Refs. [53].

B. SNe Ia sample

As formerly discussed, in order to perform our test, we need the luminosity distance for each galaxy cluster. To achieve this, we consider the PANTHEON dataset of Type Ia supernovae, compiled in 2018 by Scolnic et al. [67], which combines observations from three subsets: 279 Type Ia supernovae from Pan-STARRS ($0.03 < z < 0.68$), samples from SDSS, SNLS, and various low- z samples from HST. This data set forms one of the largest combined sets of Type Ia supernovae, totaling 1048 events with redshift intervals ranging from 0.01 to 2.26. The luminosity distance (d_L) calculated for this sample is obtained by considering H_0 as provided by reference [66] and as done in previous works [54] where $H_0 = 67.36 \pm 0.54$ km/s/Mpc. To determine the luminosity distance for each galaxy

⁷ Which would be equivalent to the modified equation for f_{gas} .

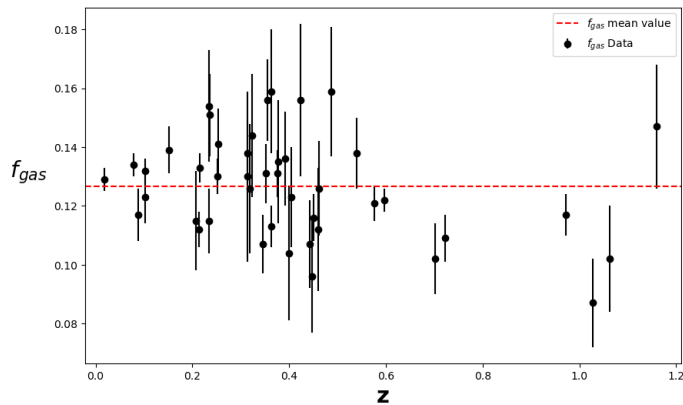


FIG. 1: The 40 Chandra X-ray gas mass fraction as a function of redshift compiled by Mantz et al. [53].

cluster, we employ the Gaussian process methodology to compute the central value along with its associated variance. The results of the Gaussian process regression for d_L are shown in Fig. 2.

In the following sections, we present the main aspects of the 2HDM to be addressed in this work and translate the above analysis to constrain the μ variation with redshift. This exemplifies how our approach can place bounds on Particle Physics models.

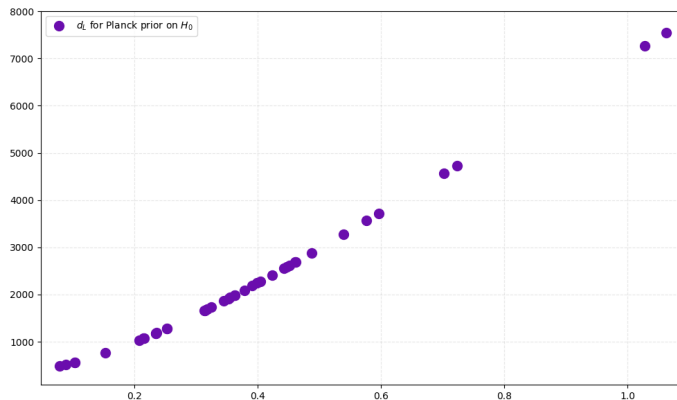


FIG. 2: Luminosity distances for the 40 galaxy clusters obtained through gaussian process regression using the value for the Hubble constant, $H_0 = 67.36 \pm 0.54$ km/s/Mpc, as given by Ref. [66].

IV. THE TWO HIGGS DOUBLET MODEL

The 2HDM [36, 37] consists of introducing an additional scalar to the SM spectrum, transforming as a doublet under the weak isospin group and carrying hypercharge $Y = +1$. As usual, we choose the vev of both doublets to be along the direction of weak isospin $T^3 = -1/2$, the electrically neutral field components, so that expansion around the minimum energy configuration $\langle \Phi_i \rangle_0$ reads,

$$\Phi_i = \begin{pmatrix} \phi_i^+ \\ \phi_i^0 \end{pmatrix} = \begin{pmatrix} \phi_i^+ \\ \frac{1}{\sqrt{2}}(v_i + \rho_i + i\eta_i) \end{pmatrix}, \quad \langle \Phi_i \rangle_0 = \begin{pmatrix} 0 \\ v_i/\sqrt{2} \end{pmatrix}, \quad i = 1, 2, \quad (8)$$

where ϕ_i^+ represents the electrically charged weak scalar eigenstates, while ρ_i and η_i are the neutral ones. The vevs are constrained by, $v = \sqrt{v_1^2 + v_2^2} = 246$ GeV, once both contribute to the gauge bosons' masses. In order to obtain

a simplified scalar potential, we introduce a discrete symmetry for the scalar doublets⁸, $Z_2 : \Phi_1 \rightarrow -\Phi_1, \Phi_2 \rightarrow \Phi_2$. Then, allowing only a bilinear, $\Phi_1^\dagger \Phi_2 + \text{h.c.}$ term, which softly breaks the Z_2 symmetry so as to avoid the domain wall problem [68], the most general renormalizable, gauge, Lorentz and CP invariant scalar potential is written as,

$$V(\Phi_1, \Phi_2) = m_1^2 \Phi_1^\dagger \Phi_1 + m_2^2 \Phi_2^\dagger \Phi_2 - m_{12}^2 (\Phi_1^\dagger \Phi_2 + \Phi_2^\dagger \Phi_1) + \frac{\lambda_1}{2} (\Phi_1^\dagger \Phi_1)^2 + \frac{\lambda_2}{2} (\Phi_2^\dagger \Phi_2)^2 \\ + \lambda_3 (\Phi_1^\dagger \Phi_1) (\Phi_2^\dagger \Phi_2) + \lambda_4 (\Phi_1^\dagger \Phi_2) (\Phi_2^\dagger \Phi_1) + \frac{\lambda_5}{2} [(\Phi_1^\dagger \Phi_2)^2 + (\Phi_2^\dagger \Phi_1)^2], \quad (9)$$

where λ_j are dimensionless parameters and m_1, m_2 and m_{12} possess mass dimension one. After the electroweak spontaneous symmetry breaking (SSB), we see that the scalars' mass terms in the potential, Eq. (9), are not in a diagonal basis, so we need to rotate these fields to their mass eigenstates in order to obtain the mass spectrum of the model. From the original eight scalars, three of them are Goldstone bosons, G and G^\pm , which are absorbed by the massive gauge bosons, Z^0 and W^\pm , respectively. The five remaining scalars get mixed to provide the mass eigenstates, namely, two CP-even scalars, h and H , one CP-odd scalar, A (these three scalars are electrically neutral), and two electrically charged ones, H^\pm . This physical basis (mass basis) is achieved through the following rotations [69],

$$\begin{pmatrix} h \\ H \end{pmatrix} = R(\alpha) \begin{pmatrix} \rho_1 \\ \rho_2 \end{pmatrix}, \quad \begin{pmatrix} G \\ A \end{pmatrix} = R(\beta) \begin{pmatrix} \eta_1 \\ \eta_2 \end{pmatrix}, \quad \begin{pmatrix} G^\pm \\ H^\pm \end{pmatrix} = R(\beta) \begin{pmatrix} \phi_1^\pm \\ \phi_2^\pm \end{pmatrix}. \quad (10)$$

Where, each of the rotation matrices, $R(\theta)$, with $\theta = \alpha, \beta$ can be written as,

$$R(\theta) \equiv \begin{pmatrix} \cos \theta & \sin \theta \\ -\sin \theta & \cos \theta \end{pmatrix}, \quad (11)$$

with

$$\tan(2\alpha) \equiv \frac{-2m_{12}^2 v_1 v_2 + 2\lambda_{345} v_1^2 v_2^2}{m_{12}^2 (v_2^2 - v_1^2) + \lambda_1 v_1^3 v_2 - \lambda_2 v_1 v_2^3}; \quad \tan \beta \equiv \frac{v_2}{v_1}, \quad (12)$$

where we have defined $\lambda_{345} \equiv \lambda_3 + \lambda_4 + \lambda_5$.

The scalar's mass spectrum then becomes:

$$m_h^2 = \frac{1}{2}(\Delta_\rho - \delta_\rho); \quad m_H^2 = \frac{1}{2}(\Delta_\rho + \delta_\rho); \quad m_A^2 = \left[\frac{m_{12}^2}{v_1 v_2} - \lambda_5 \right] (v_1^2 + v_2^2); \quad (13)$$

$$m_{H^\pm}^2 = \left[\frac{m_{12}^2}{v_1 v_2} - \frac{1}{2}(\lambda_4 + \lambda_5) \right] (v_1^2 + v_2^2), \quad (14)$$

where we have defined,

$$\Delta_\rho = \frac{m_{12}^2 (v_1^2 + v_2^2)}{v_1 v_2} + \lambda_1 v_1^2 + \lambda_2 v_2^2 \quad \text{and} \quad \delta_\rho = \left[\left(\frac{m_{12}^2 (v_1^2 - v_2^2)}{v_1 v_2} - \lambda_1 v_1^2 + \lambda_2 v_2^2 \right)^2 + 4(m_{12}^2 - \lambda_{345} v_1 v_2)^2 \right]^{\frac{1}{2}}.$$

In the above description, it becomes evident that the neutral CP-even mass hierarchy is $m_H > m_h$. For our purposes, the relevant interactions for future computations (electron mass, anomalous magnetic moment of the muon) come from the Yukawa Lagrangian,

$$-\mathcal{L}_Y = y_{ij}^{1e} (\bar{L}^i \Phi_1) e_R^j + y_{ij}^{1d} (\bar{Q}^i \Phi_1) d_R^j + y_{ij}^{1u} (\bar{Q}^i \tilde{\Phi}_1) u_R^j \\ + y_{ij}^{2e} (\bar{L}^i \Phi_2) e_R^j + y_{ij}^{2d} (\bar{Q}^i \Phi_2) d_R^j + y_{ij}^{2u} (\bar{Q}^i \tilde{\Phi}_2) u_R^j + \text{h.c.}, \quad (15)$$

where each term is summed over the family indices i and j and we defined $\tilde{\Phi}_i \equiv i\sigma_2 \Phi_i^*$. In this expression, L_i and Q_i represent the usual Standard Model (SM) left-handed lepton and quark doublets, respectively, while e_R, u_R , and d_R denote their corresponding right-handed singlet partners. The parameters y_{ij} denote the matrix elements

⁸ This symmetry will soon be conveniently used to restrict the interaction of leptons with only one of the scalar multiplets.

(not necessarily diagonal) of the dimensionless Yukawa couplings. After the spontaneous symmetry breaking, this Lagrangian leads to the following fermionic mass matrix elements :

$$M_{ij}^f = \frac{v_1}{\sqrt{2}} y_{ij}^{1f} + \frac{v_2}{\sqrt{2}} y_{ij}^{2f}, \quad (16)$$

with the index f denoting a quark or a lepton with the same weak isospin.

Observe that, differently from the SM, here we have two unrelated sources of contributions to fermion mass terms, one from the matrix $v_1 y^{1f}$ and another from $v_2 y^{2f}$. The bold implication is that there is no change of basis that diagonalizes both terms simultaneously, leading to Flavor Changing Neutral Currents (FCNC) in the fermion-scalar couplings. The fact that such interactions are experimentally unobserved calls for some arrangement to strongly suppress them. This can be achieved if we demand that each fermion mass matrix comes from only one of the scalar doublets, so that diagonalizing all fermion mass matrices, M^f , implies the automatic diagonalization of $y^{1,2}$ (with the corresponding change from fermion interaction eigenstates to mass eigenstates) and, consequently, the disappearance of FCNC. This mechanism is known as Natural Flavor Conservation (NFC) [70, 71]. The easiest way to implement that is through the introduction of an extra symmetry, under which the scalar doublets transform differently, so that each fermion (also transforming under this symmetry) can couple to only one of the doublets. Our choice for that is a discrete Z_2 symmetry such that, $\Phi_1 \rightarrow -\Phi_1$, $\Phi_2 \rightarrow \Phi_2$. This is the reason we omitted odd terms in either of the scalar doublets in the scalar potential, Eq. (9), except for the soft Z_2 breaking term as we mentioned before.

The convention is to take all the fermion doublets, as well as singlet up-type quarks (u_R), to transform trivially, so that the up-type quarks always couple to Φ_2 and we are left to decide which of the scalar doublets couples to the singlet down-type fermions (right-handed down-type quarks d_R and charged leptons e_R). In the scenario we choose to work here, called **lepton-specific** 2HDM (or LS2HDM for short), d_R is assigned positive parity under Z_2 (so that both, d_R and u_R couple to Φ_2 , only) and e_R is assigned negative parity (couples to Φ_1 , only). The main reason for choosing LS2HDM is because we restrict the electron to receive mass from one vev and the quarks from the other. In this way, we will have the simplest configuration regarding the variation of vevs with redshift (or, equivalently, $\tan \beta$), that is, we need to analyze only the case in which only one of the vevs varies, v_1 , as a consequence of the variation of the gas mass fraction to be analyzed in the next section. We can then rewrite the Yukawa Lagrangian, Eq. (15), in the mass basis for both, scalars and fermions [69],

$$\begin{aligned} -\mathcal{L}_Y = & \sum_{f=u,d,e} m_f \bar{f} f + \sum_{f=u,d,e} \frac{m_f}{v} (\xi_h^f \bar{f} f h + \xi_H^f \bar{f} f H - i \xi_A^f \bar{f} \gamma_5 f A) \\ & - \left[\frac{\sqrt{2}}{v} \bar{u} V_{ud} (m_u \xi_A^u P_L + m_d \xi_A^d P_R) d H^+ + \frac{\sqrt{2} m_e \xi_A^e}{v} \bar{\nu}_L e_R H^+ + \text{h.c.} \right], \end{aligned} \quad (17)$$

with,

$$\xi_h^u = \xi_h^d = s_\alpha / s_\beta, \quad \xi_h^e = c_\alpha / c_\beta, \quad \xi_H^u = \xi_H^d = c_\alpha / s_\beta, \quad \xi_H^e = -s_\alpha / c_\beta, \quad \xi_A^u = -\xi_A^d = (t_\beta)^{-1}, \quad \xi_A^e = t_\beta,$$

where we defined $c_\theta \equiv \cos \theta$, $s_\theta \equiv \sin \theta$ and $t_\theta \equiv \tan \theta$ for shorthand notation, the sum is over all up-type and down-type fermions (leptons and quarks) and the coefficient V_{ud} denotes the appropriate element of the CKM matrix. There is a linear combination of the neutral scalars that corresponds to the SM Higgs boson [69],

$$H^{\text{SM}} \sim h \cos(\beta - \alpha) + H \sin(\beta - \alpha) \quad (18)$$

which allows us to choose between h and H to represent the observed Higgs boson, H^{SM} , with mass around 125 GeV, and consistent with SM predictions for its interactions with fermions, implying a constraint on the mixing angles α and β . Here we make the choice of h , the lighter scalar, to be the observed Higgs boson, so that $\alpha = \beta$, from now on. We are now prepared to obtain a constraint on this model from the bounds on μ varying with the redshift as inferred from the gas mass fraction in galaxy clusters, as we present next.

V. ANALYSIS AND RESULTS

Now we are going to obtain bounds on the variation of the electron to proton mass ratio by comparing the observed gas mass fraction within galaxy clusters to the theoretical gas mass fraction which is predicted by cosmological models as explained earlier in Sec. II. From the 40 data points we inferred a variation of μ ($\Delta\mu$), as follows: we take consecutive values of μ obtained from the data shown in table II (see the appendix) and subtract them $\Delta\mu = \mu_{j+1} - \mu_j$ so we

have $j-1$ values of $\Delta\mu$, and the mean value is taken to be the expected variation of $\Delta\mu$ in this redshift span. We find that value to be:

$$\Delta\mu = -6.3 \cdot 10^{-3} \pm 2.7 \cdot 10^{-1}. \quad (19)$$

Although the constraints are not as restrictive as those obtained through quasar absorption spectra, the measurements are in agreement within 1σ confidence level. It is worth noting that the physics involved here is completely different. The techniques used to measure $\mu(z)$ in quasar spectroscopy rely on the hyperfine transition of molecules such as H_2 , FeII , and SiII [72, 73], with this transition being proportional to the ratio $\frac{\alpha_{EM}^2 g_p}{\mu}$ and the effective radius of the nucleus. In this scenario, the ratio between the mass of the electron and the mass of the proton is not directly measured; rather, it is the ratio between the mass of the electron and the effective mass of the nucleus [12]. A measurement using the Eq. (4) obtained through X-ray emission from ICM plasma, which consists predominantly of hydrogen ions, is a more direct measurement.

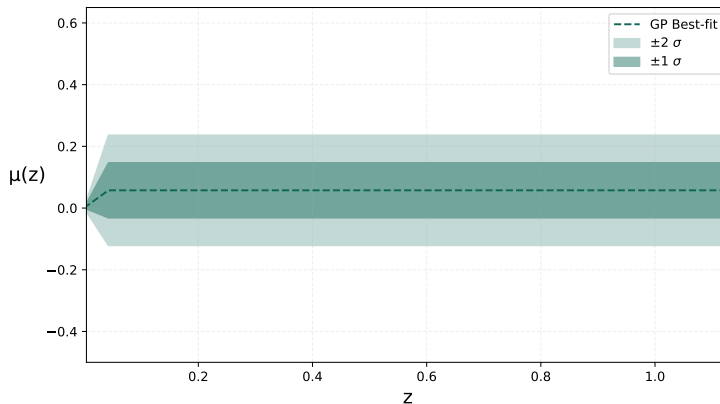


FIG. 3: Reconstruction of $\mu(z)$ via gaussian processes regression by using the values from the Table II. The dashed line represents the best-fit curve, while the dark green region corresponds to the 1σ confidence interval, and the light green region represents the 2σ confidence interval.

Now, in order to obtain $\mu(z=0)$ from the observational values shown in Table II, we apply a Gaussian process to those values (hereafter, we shall refer to it as $\mu_{\text{GPR}}(0)$). Gaussian Processes (GPs) offer a method for reconstructing a function from observational data without assuming a specific parametrization. The GP reconstruction process involves selecting a prior mean function and a covariance function that quantifies the correlation between the values of the dependent variable in the reconstruction, which are characterized by a set of hyperparameters such as the signal variance σ and the characteristic length scale l . Unlike regular parameters, hyperparameters do not dictate the shape of a function; rather, they characterize typical variations in the reconstructed function. l roughly represents the scale over which significant changes occur in the function values across z , while σ indicates the typical magnitude of these alterations [74][75]. While more complex covariance functions may involve additional hyperparameters, in this work we used a covariance function that solely incorporate σ and l . To reconstruct $\mu(z)$, we do not specify a prior on μ to avoid any additional assumptions, we also optimize our kernel parameters via random search to avoid overfitting the model. We show the plot of our reconstruction in Fig. 3 along with a Gaussian kernel serving as the covariance function, as follows,

$$k(z, z') = \sigma^2 \exp\left(-\frac{(z - z')^2}{2l^2}\right). \quad (20)$$

To perform the GP we used the Python scientific package scikit-learn [76].

Finally, we define a likelihood function that compares the values of $\mu(z)$ obtained by GPR (μ_{GPR}) taken when $z=0$, with the experimentally measured value (fiducial) μ (μ_{fid}),

$$L(y_e, v_2, \cot\beta(z)) = \prod_{i=1}^n \frac{1}{\sqrt{2\pi\sigma_i^2}} \exp\left(-\frac{(\mu_{\text{GPR}}(z_i) - \mu_{\text{fid}}(z_i))^2}{2\sigma_i^2}\right), \quad (21)$$

to transition from the likelihood function $L(y_e, v_2, \cot\beta(z))$ to its logarithmic form $\log L$, we focus on $z=0$, where the likelihood reduces to a single comparison between the Gaussian Process Regression (GPR) prediction $\mu_{\text{GPR}}(0)$

and the experimental value $\mu_{\text{fid}}(0)$. The parameter $\mu(z)$, defined as the ratio of the electron to proton mass in the two-Higgs-doublet model, incorporates $\cot\beta(z) = v_1/v_2$, which is assumed to vary with z . By fixing $z = 0$, the likelihood simplifies to a Gaussian form, allowing for a direct calculation of $\log L$ for statistical purposes.

$$\log L = -\frac{1}{2} \log(2\pi\sigma^2) - \frac{1}{2} \left(\frac{\mu_{\text{GPR}}(0) - \mu_{\text{fid}}(0)}{\sigma} \right)^2. \quad (22)$$

We initialized the ensemble by choosing an initial value for the electron Yukawa coupling, y_e , as $1 \times 10^{-3} \pm$ some gaussian noise of order 10^{-4} . Similarly, the ratio of vevs in the LS2HDM, $\cot\beta(z)$, was initialized as $1/50$, with the noise term ensuring diversity in the initial values across the ensemble. Furthermore, v_2 values were sampled from a Gaussian distribution centered at 240.5. These initial conditions were then used to start the MCMC process. Using the diagonalized Yukawa coupling for electrons in the LS2HDM, obtained from Eqs. (15,16), and assuming that any variation in μ with z arises from $v_1(z)$, that is, the vev responsible for the electron mass, while the proton mass remains constant, we obtain,

$$\mu_{\text{fid}}(z) = \frac{y_e v_2}{\sqrt{2} m_p (\Lambda_{\text{QCD}})} \cot\beta(z). \quad (23)$$

This expression, evaluated at $z = 0$, provides constraints for the Yukawa coupling of the electron, y_e , for the $\cot\beta_0$, and the vev, v_2 we use in the log-likelihood from equation Eq.(22). The samples generated provide us with the best estimates for the parameters as given in Fig. 4, along with the conditional 2D regions for the confidence intervals. The results for the constrained parameters are summarized in Table I.⁹

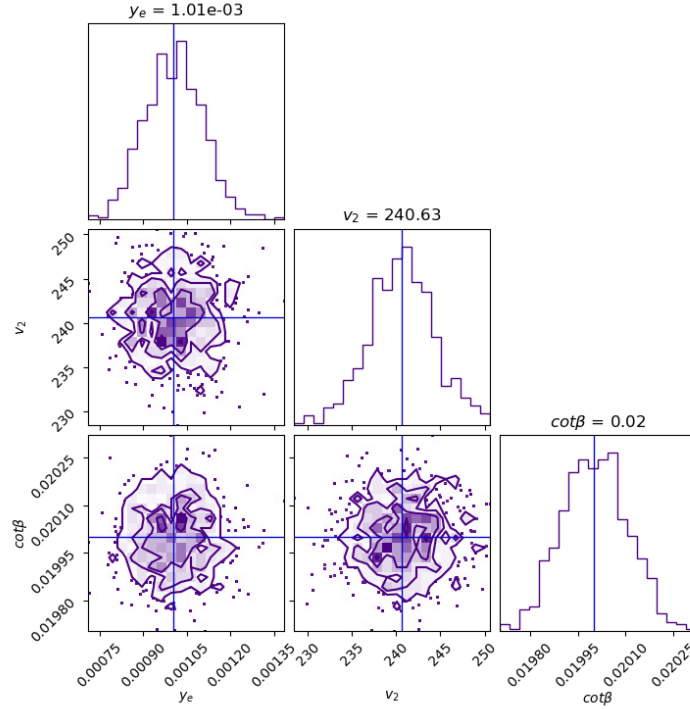


FIG. 4: Constraints on y_e , v_2 , and $\cot\beta$ from $\mu(z)$ obtained using Plank's prior. The diagonal plots represent 1-D marginalized likelihood distributions of each parameter present and off-diagonal contours are 68%, 95%, and 99% 2-D marginalized confidence regions.

This constitutes the main result of our work. Next, we compute the contribution of LS2HDM to the muon anomalous magnetic moment and gather additional constraints to the model so as to find the favorable parameter space that is constrained by $\mu(z)$.

⁹ We provide the source code for the replication of our analysis in the link for github repository: [2HDM](#).

Parameter	Value
y_e	$(1.01 \pm 0.07) \cdot 10^{-3}$
v_2 (GeV)	240.57 ± 2.93
$\cot \beta$	$(2.003 \pm 0.081) \cdot 10^{-3}$

TABLE I: Summary of the best values for the model's parameters obtained from our MCMC sampling.

VI. LS2HDM AND THE MUON ANOMALOUS MAGNETIC MOMENT

There is, currently, a discrepancy between the muon anomalous magnetic moment, $a_\mu \equiv (g-2)_\mu$, predicted by the SM and its experimental value, $\Delta a_\mu^{obs} \equiv a_\mu^{EXP} - a_\mu^{SM} = (25.1 \pm 5.9) \cdot 10^{-10}$ [34, 35]. We show here that our model is capable of accounting for that difference at 2σ .

The most important contributions to $(g-2)_\mu$ from the LS2HDM are given by the diagrams in Fig. 5, with ϕ representing the neutral scalars h , H , A . Here, h is chosen to be the SM Higgs, with mass, $m_h = 125$ GeV, whose contribution is already considered in the theoretical prediction so it does not enter in the computation of the deviation. Furthermore, the charged scalar contribution is insignificant, so it will not be considered here, meaning that we only take H and A into account. The first one loop diagram in Fig. 5 results in [77],

$$\Delta a_\mu^{1 \text{ loop}} = \frac{1}{8\pi^2} \left(\frac{m_\mu}{v} \right)^2 \left\{ (\xi_H^\mu)^2 \left[2I_1 \left(\frac{m_\mu^2}{m_H^2} \right) - I_2 \left(\frac{m_\mu^2}{m_H^2} \right) \right] - (\xi_A^\mu)^2 I_2 \left(\frac{m_\mu^2}{m_A^2} \right) \right\}, \quad (24)$$

with,

$$\begin{aligned} I_1(x) &= 1 + \frac{1-2x}{2x\sqrt{1-4x}} \ln \left(\frac{1+\sqrt{1-4x}}{1-\sqrt{1-4x}} \right) + \frac{1}{2x} \ln x \\ &\approx x \left(-\frac{3}{2} - \ln x \right) + x^2 \left(-\frac{16}{3} - 4 \ln x \right) + \mathcal{O}(x^3), \end{aligned} \quad (25)$$

$$\begin{aligned} I_2(x) &= \frac{1}{2} + \frac{1}{x} + \frac{1-3x}{2x^2\sqrt{1-4x}} \ln \left(\frac{1+\sqrt{1-4x}}{1-\sqrt{1-4x}} \right) + \frac{1-2x}{2x^2} \ln x \\ &\approx x \left(-\frac{11}{6} - \ln x \right) + x^2 \left(-\frac{89}{12} - 5 \ln x \right) + \mathcal{O}(x^3). \end{aligned} \quad (26)$$

At one loop, H contributes positively, and A contributes negatively [78], so that the overall contribution is not enough to explain the anomaly. For this reason we include the second diagram in Fig. 5, a special type of two loop contribution called Barr-Zee diagram, which yields [77],

$$\Delta a_\mu^{\text{Barr-Zee}} = -\frac{2\alpha}{\pi} \frac{1}{8\pi^2} \left(\frac{m_\mu}{v} \right)^2 \sum_f N_c^f Q_f^2 \left\{ \xi_H^\mu \xi_H^f f \left(\frac{m_f^2}{m_H^2} \right) - \xi_A^\mu \xi_A^f g \left(\frac{m_f^2}{m_A^2} \right) \right\} \quad (27)$$

$$f(z) = \frac{z}{2} \int_0^1 dx \frac{1-2x(1-x)}{x(1-x)-z} \ln \left(\frac{x(1-x)}{z} \right) \quad (28)$$

$$g(z) = \frac{z}{2} \int_0^1 dx \frac{1}{x(1-x)-z} \ln \left(\frac{x(1-x)}{z} \right) \quad (29)$$

Here H contributes negatively, and A contributes positively [78]. We sum over all the fermions, f , in the loop, each one characterized by its color number, N_c^f (which is equal to 3 for quarks and zero for leptons), and its electric charge (multiple of unit positron charge), Q_f .

The above expressions depend on m_H , m_A and $\tan \beta$, which are in principle hard to constrain because (considering $\beta = \alpha$) the quark couplings from Eq. (17) are proportional to $\cot \beta \ll 1$. This means that hadronic cross sections are attenuated and thus incapable of providing bounds for the 2HDM masses. So it becomes necessary to establish

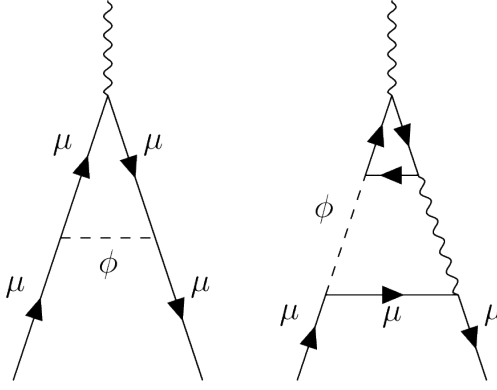


FIG. 5: Neutral scalar contributions to muon, $(g-2)_\mu$ (the wiggly lines are photon ones).

model-dependent bounds on these parameters, and it is this feature that reveals the importance of new fronts to obtain these bounds, like the electron varying mass inferred from the electron to proton mass ratio, μ , discussed in the previous sections. We follow here the model suggested by Ref. [78], which uses lepton universality constraints, the CDF W boson mass results and muonic $g-2$ measurements to probe the allowed parameter space (as well as the requirement of vacuum stability, perturbativity and unitarity in the wrong sign scenario). The $h \rightarrow AA$ decay channel is considered, adding the constraint $m_h \geq 2m_A$.

The regions in parameter space that meet these requirements and keep $\Delta a_\mu^{2\text{HDM}}(m_H, m_A, t_\beta) = \Delta a_\mu^{1\text{ loop}} + \Delta a_\mu^{\text{Barr-Zee}}$ inside 1σ , 2σ or 3σ deviation from $\Delta a_\mu^{\text{obs}} = (25.1 \pm 5.9) \cdot 10^{-10}$ are shown in Figs. 6 and (7), displayed as green bands. In Fig. 6, we present the predictions of $\tan \beta$ against the pseudoscalar mass, m_A , keeping the mass of the heavier scalar, m_H , fixed at $m_H = 300$ GeV. We take into account the bounds stemming from our astrophysical analysis of $\mu(z)$ in Table I, representing $\cot \beta = 0.02003 \pm 0.00081$ (light gray band). We see that a light pseudoscalar is favored, with mas ranging from around 10 to 50 GeV. As for the Fig. 7, our prediction for $\Delta a_\mu^{2\text{HDM}}$ is plotted as a function of m_A with $m_H = 300$ GeV. We kept $\tan \beta$ fixed with central value $\tan \beta = 49.92$ (solid purple curve) and the limiting values at $\pm 1\sigma_{\tan \beta} = \pm 2.02$ (dashed purple curves). The green bands are the observed $(g-2)_\mu$ discrepancy at 1σ , 2σ and 3σ . From this figure we conclude that the neutral scalar contributions can solve the muon anomaly at 1σ when $m_A \gtrsim 10$ GeV. The critical point at $m_A \approx 10.67$ GeV is due to the competition between the one loop (negative) and Barr-Zee (positive) contributions.

Just for completeness, we use some additional constraints from Ref. [78] that give $m_{H^\pm} \gtrsim m_H$, besides solving the $(g-2)_\mu$ discrepancy and the W mass anomaly simultaneously. For that, we superpose our results from the $\mu(z)$ bounds on $\tan \beta$ in the LS2HDM (table I) to their results on $(g-2)_\mu$, universality tests through τ -decay and $Z \rightarrow \bar{l}l$ (Z decay into a pair of leptons), as well as the scalar mass difference, $\Delta \equiv m_{H^\pm} - m_H$, constrained by the requirement that it solves the W mass anomaly [79]. We see from Fig. 8 that these extra bounds are compatible with our constraints on $\tan \beta$ in the 1σ range $47.9 \leq \tan \beta \leq 51.9$, covering the central value obtained before with a small variation depending on the heavier neutral scalar mass. The first panel in that figure is for a heavier Higgs, $m_H = 300$ GeV, while the second one is for $m_H = 400$ GeV. The upper bounds on $\tan \beta$ from τ -decay and $Z \rightarrow \bar{l}l$ are shown as full and dashed lines for different choices of the scalar mass difference, Δ . Observe that their results for the $(g-2)_\mu$, sketched in brown, is a little bit different from ours because they use only the lepton τ in the Barr-Zee loop, while we summed over all the SM fermions.

VII. CONCLUSIONS

In this work, we analyze the expression for the gas mass fraction of a galaxy cluster and found that $f_{\text{gas}} \propto (1 + \mu)^2$. Thus, by combining Type Ia Supernovae observations with gas mass fraction measurement data from 40 galaxy clusters, we imposed constraints on a possible variation of the electron-to-proton mass ratio, $\Delta\mu$, as given in Eq. (19). Additionally, using a Gaussian regression process, we reconstructed a $\mu(z)$ curve, as given in Eq. (23), which allows us to impose limits on models beyond the electroweak Standard Model (SM) of particle physics.

To illustrate our approach, we employed a specific extension of the scalar sector of the SM by adding an extra Higgs doublet and an additional discrete Z_2 symmetry. This resulted in the two-Higgs doublet model in the scenario of lepton-specific coupling, which we referred to as LS2HDM, presented in Sec. IV. This choice was made not only for simplicity but also to give meaningful context to a well-studied class of models in the literature. We were able to translate the results on $\mu(z)$ into constraints on the parameters of the model, namely $\cot \beta$ (reverted to $\tan \beta$), v_2 ,

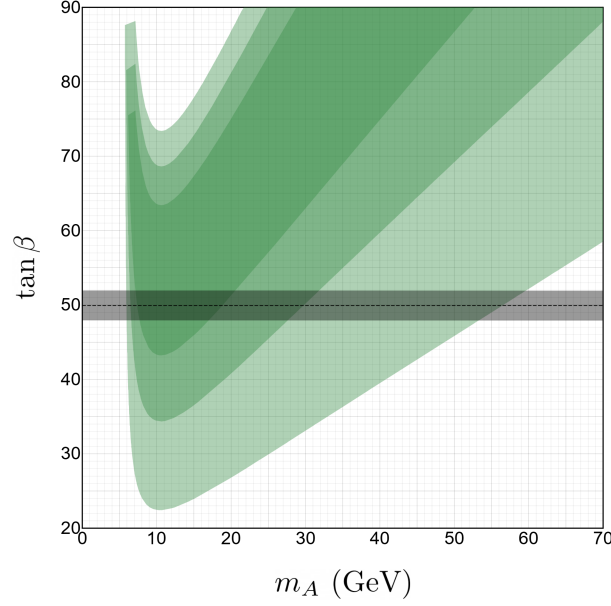


FIG. 6: Constraints on 2HDM parameters m_A and $\tan \beta$ using the $(g-2)_\mu$ prediction of LS2HDM (m_H is fixed at 300 GeV). The green regions represent, from darker to lighter, 1σ , 2σ and 3σ , where a χ^2 distribution is adopted. The region in light gray represents $\cot \beta = 0.02003 \pm 0.00081$ from Table I.

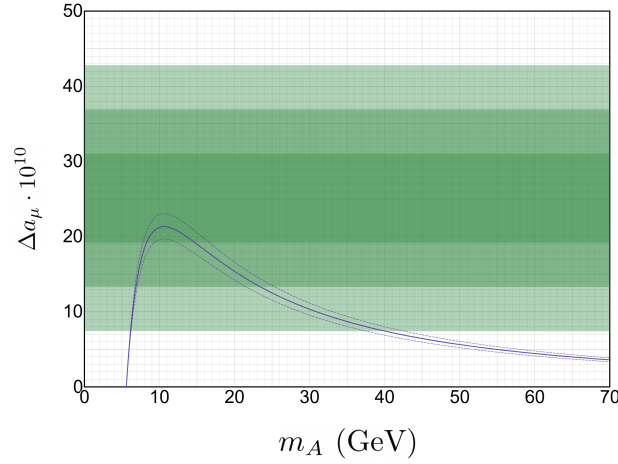


FIG. 7: $\Delta a_\mu^{2\text{HDM}}$ as a function of m_A with $m_H = 300$ GeV. We took the central value $\tan \beta = 49.92$ (solid purple curve) and the limiting values at $1\sigma_{\tan \beta} = 2.02$ (dashed purple curves). The green bands are the observed $(g-2)_\mu$ discrepancy at 1σ , 2σ and 3σ .

and y_e (see Table I), finding their optimal values through MCMC sampling.

These constraints, when further compared with the model's ability to account for the discrepancy between experimental and SM theoretical values of the anomalous muon magnetic moment, $(g-2)_\mu$, resulted in a robust set of bounds on the parameters. This analysis favored a relatively light pseudoscalar, with $m_A \gtrsim 10$ GeV, and a heavier scalar with mass around $300 \leq m_H \leq 400$ GeV. These conclusions were obtained by combining existing bounds [78] on the model, including constraints from τ -decay and $Z \rightarrow \ell\bar{\ell}$, along with the accommodation of the W-mass anomaly observed by the CDF collaboration [79].

Finally, we emphasize that the main goal of this work was to explore a complementary approach to Particle Physics models at the interface with Astrophysics and Cosmology. In our case, this approach was derived from the properties

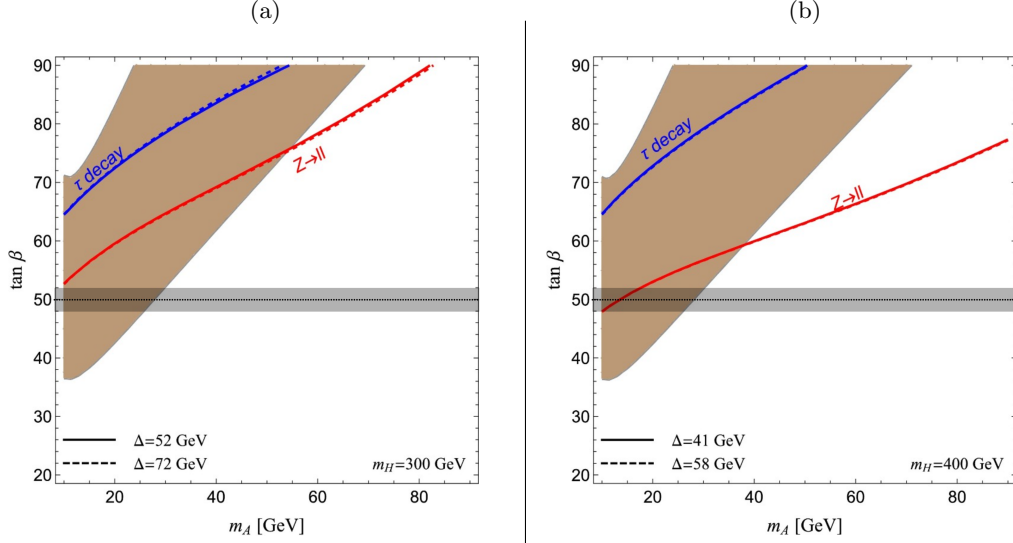


FIG. 8: (a) - (b) Constraints given by [78]. The 2σ region allowed by the muon $g - 2$ is sketched in brown. The colored lines give upper bounds on $\tan \beta$ from lepton universality tests, exploring both τ decay and Z decay in any pair of leptons. The full and dashed lines are associated with the lower and upper bounds on $\Delta \equiv m_{H^\pm} - m_H$, respectively, and we superimposed the region in light gray to represent our astrophysical results. In Fig. 8a, m_H is fixed at 300 GeV and Δ ranges from 52 to 72 GeV. In Fig. 8b, m_H is fixed at 400 GeV and Δ ranges from 41 to 58 GeV.

of gas in galaxy clusters. Our results highlight the importance of seeking new constraints for non-standard physics in environments beyond particle physics accelerators, as can be readily seen in Figs. 8a and 8b, where the allowed parameter space has been further reduced to the gray range when our astrophysical analysis is taken into account. Admittedly, we restricted ourselves to a very specific model, but it served our purpose of demonstrating that new paths can be followed to unite these areas, without evident correlation, with great gain for model building in Particle Physics, confirming that the large-scale structures of the universe may contain more information than previously anticipated. In the coming years, there will be a significant increase in the quantity and quality of observations made possible by instruments such as the eROSITA telescope, a Russian-German collaboration. This progress will allow more comprehensive statistical analyses, making it feasible to reach more restrictive limits using the methodology described in this paper.

Acknowledgments

PSRS would like to thank the financial support from Conselho Nacional de Desenvolvimento Científico e Tecnológico (CNPq) under the project No. 309650/2019-4 and the support of UFPB through an internal project PIA16656-2023; RFLH thanks the financial support from the Conselho Nacional de Desenvolvimento Científico e Tecnológico (CNPq) under the project No. 308550/2023-47; RGA thanks the financial support from UFPB through PIBIC-CNPq under the project No. PIA16656-2023.

Appendix A: 40 observations of μ

The function `delta_mu_with_error` in **2HDM** calculates the differences between the values of μ at consecutive positions and their respective uncertainties. The formula for each $\Delta\mu$ is given by: $\Delta\mu_i = \mu_{i+1} - \mu_i$. And for the associated error of each $\Delta\mu_i$, we have $\Delta\sigma_{\mu_i} = \sqrt{\sigma_{\mu_{i+1}}^2 + \sigma_{\mu_i}^2}$. Finally, for the $\Delta\mu \equiv \langle\Delta\mu\rangle$

$$\langle\Delta\mu\rangle = \frac{1}{n} \sum_{i=1}^n \Delta\mu_i \quad (\text{A1})$$

where $\Delta\mu_i$ are the differences of μ and n is the total number of values. We use the $\langle\Delta\mu\rangle$ as our estimate for $\Delta\mu$ in Eq. (19)

μ	σ_μ
0.078	0.259413
0.088	0.203252
0.103	0.115985
0.103	0.143774
0.152	0.095311
0.208	-0.015405
0.214	-0.025265
0.215	-0.029885
0.235	0.102452
0.235	0.050020
0.236	0.062295
0.252	0.020226
0.253	0.109813
0.313	0.093470
0.314	0.044570
0.318	0.069704
0.324	0.078395
0.345	-0.044600
0.352	-0.007903
0.355	0.129140
0.363	0.156912
0.363	-0.024807
0.378	0.103819
0.391	0.080763
0.399	-0.087368
0.404	-0.021369
0.423	0.215044
0.442	-0.074786
0.447	-0.079323
0.451	0.013216
0.460	0.013755
0.461	0.039923
0.487	0.135969
0.539	0.134061
0.576	0.043878
0.596	0.189276
0.702	-0.146335
0.723	0.184268
1.028	0.013755
1.063	0.011109

TABLE II: Data from 40 observations of μ as obtained from Eq. (7)

-
- [1] P. A. M. Dirac, *Nature* volume **139**, 323 (1937).
 - [2] V. A. Dzuba, V. V. Flambaum, and J. K. Webb, *Phys. Rev. A* **59**, 230 (1999), URL <https://link.aps.org/doi/10.1103/PhysRevA.59.230>.
 - [3] Y. Fujii, A. Iwamoto, T. Fukahori, T. Ohnuki, M. Nakagawa, H. Hidaka, Y. Oura, and P. Möller, *Nuclear Physics B* **573**, 377–401 (2000), ISSN 0550-3213, URL [http://dx.doi.org/10.1016/S0550-3213\(00\)00038-9](http://dx.doi.org/10.1016/S0550-3213(00)00038-9).
 - [4] V. V. Flambaum and A. F. Tedesco, *Phys. Rev. C* **73**, 055501 (2006), URL <https://link.aps.org/doi/10.1103/PhysRevC.73.055501>.
 - [5] K. A. Olive, M. Pospelov, Y.-Z. Qian, G. Manhès, E. Vangioni-Flam, A. Coc, and M. Cassé, *Phys. Rev. D* **69**, 027701 (2004), URL <https://link.aps.org/doi/10.1103/PhysRevD.69.027701>.
 - [6] A. F. M. Fiorenzano, G. Vladilo, and P. Bonifacio, *Search for alpha variation in uves spectra: Analysis of c iv and si iv doublets towards qso 1101-264* (2004), astro-ph/0312270.
 - [7] P. Tzanavaris, J. K. Webb, M. T. Murphy, V. V. Flambaum, and S. J. Curran, *Physical Review Letters* **95** (2005), ISSN 1079-7114, URL <http://dx.doi.org/10.1103/PhysRevLett.95.041301>.
 - [8] P. Molaro, M. Centurión, J. B. Whitmore, T. M. Evans, M. T. Murphy, I. I. Agafonova, P. Bonifacio, S. D’Odorico, S. A. Levshakov, S. Lopez, et al., *Astronomy & Astrophysics* **555**, A68 (2013), ISSN 1432-0746, URL <http://dx.doi.org/10.1051/0004-6361/201321351>.
 - [9] M. T. Murphy, A. L. Malec, and J. X. Prochaska, *Monthly Notices of the Royal Astronomical Society* **461**, 2461–2479 (2016), ISSN 1365-2966, URL <http://dx.doi.org/10.1093/mnras/stw1482>.
 - [10] J.-P. Uzan, *Rev. Mod. Phys.* **75**, 403 (2003), URL <https://link.aps.org/doi/10.1103/RevModPhys.75.403>.
 - [11] J. D. Barrow, *Physical Review D* **71** (2005), ISSN 1550-2368, URL <http://dx.doi.org/10.1103/PhysRevD.71.083520>.
 - [12] C. J. A. P. Martins, *Reports on Progress in Physics* **80**, 126902 (2017), ISSN 1361-6633, URL <http://dx.doi.org/10.1088/1361-6633/aa860e>.
 - [13] C. Bambi, *Search for variations of fundamental constants* (2022), 2210.11959.
 - [14] H. Wei, X.-P. Ma, and H.-Y. Qi, *Physics Letters B* **703**, 74 (2011), ISSN 0370-2693, URL <https://www.sciencedirect.com/science/article/pii/S037026931100846X>.
 - [15] T. Harko, F. S. N. Lobo, and O. Minazzoli, *Phys. Rev. D* **87**, 047501 (2013), URL <https://link.aps.org/doi/10.1103/PhysRevD.87.047501>.
 - [16] A. Hees, O. Minazzoli, and J. Larena, *Phys. Rev. D* **90**, 124064 (2014), URL <https://link.aps.org/doi/10.1103/PhysRevD.90.124064>.
 - [17] T. Damour and A. Polyakov, *Nuclear Physics B* **423**, 532–558 (1994), ISSN 0550-3213, URL [http://dx.doi.org/10.1016/0550-3213\(94\)90143-0](http://dx.doi.org/10.1016/0550-3213(94)90143-0).
 - [18] C. Martins, P. Vielzeuf, M. Martinelli, E. Calabrese, and S. Pandolfi, *Physics Letters B* **743**, 377–382 (2015), ISSN 0370-2693, URL <http://dx.doi.org/10.1016/j.physletb.2015.03.002>.
 - [19] H. Davoudiasl and P. P. Giardino, *Physics Letters B* **788**, 270–273 (2019), ISSN 0370-2693, URL <http://dx.doi.org/10.1016/j.physletb.2018.11.041>.
 - [20] D. Brzeminski, Z. Chacko, A. Dev, and A. Hook, *Phys. Rev. D* **104**, 075019 (2021), URL <https://link.aps.org/doi/10.1103/PhysRevD.104.075019>.
 - [21] S. Galli, *Physical Review D* **87** (2013), ISSN 1550-2368, URL <http://dx.doi.org/10.1103/PhysRevD.87.123516>.
 - [22] I. de Martino, C. J. A. P. Martins, H. Ebeling, and D. Kocevski, *Phys. Rev. D* **94**, 083008 (2016), URL <https://link.aps.org/doi/10.1103/PhysRevD.94.083008>.
 - [23] I. De Martino, C. J. A. P. Martins, H. Ebeling, and D. Kocevski, *Universe* **2** (2016), ISSN 2218-1997, URL <https://www.mdpi.com/2218-1997/2/4/34>.
 - [24] L. Colaço, R. Holanda, R. Silva, and J. Alcaniz, *Journal of Cosmology and Astroparticle Physics* **2019**, 014–014 (2019), ISSN 1475-7516, URL <http://dx.doi.org/10.1088/1475-7516/2019/03/014>.
 - [25] R. F. L. Holanda, V. C. Busti, L. R. Colaço, J. S. Alcaniz, and S. J. Landau, *JCAP* **2016**, 055 (2016), 1605.02578.
 - [26] L. R. Colaço, R. F. L. Holanda, R. Silva, and J. S. Alcaniz, *JCAP* **2019**, 014 (2019), 1901.10947.
 - [27] Z.-E. Liu, W.-F. Liu, T.-J. Zhang, Z.-X. Zhai, and K. Bora, *The Astrophysical Journal* **922**, 19 (2021), ISSN 1538-4357, URL <http://dx.doi.org/10.3847/1538-4357/ac2150>.
 - [28] G. Aad et al. (ATLAS), *Phys. Lett. B* **716**, 1 (2012), 1207.7214.
 - [29] S. Chatrchyan et al. (CMS), *Phys. Lett. B* **716**, 30 (2012), 1207.7235.
 - [30] G. Aad et al. (ATLAS), *Nature* **607**, 52 (2022), [Erratum: *Nature* 612, E24 (2022)], 2207.00092.
 - [31] G. Bertone and D. Hooper, *Rev. Mod. Phys.* **90**, 045002 (2018), 1605.04909.
 - [32] P. F. de Salas, D. V. Forero, S. Gariazzo, P. Martínez-Miravé, O. Mena, C. A. Ternes, M. Tórtola, and J. W. F. Valle, *JHEP* **02**, 071 (2021), 2006.11237.
 - [33] F. Capozzi, E. Di Valentino, E. Lisi, A. Marrone, A. Melchiorri, and A. Palazzo, *Phys. Rev. D* **95**, 096014 (2017), [Addendum: *Phys.Rev.D* 101, 116013 (2020)], 2003.08511.
 - [34] L. Cotrozzi and M. Sorbara, in *Proceedings of 41st International Conference on High Energy physics — PoS(ICHEP2022)* (2022), vol. 414, p. 749.
 - [35] A. Keshavarzi, K. S. Khaw, and T. Yoshioka, *Nuclear Physics B* **975**, 115675 (2022), ISSN 0550-3213, URL <http://dx.doi.org/10.1016/j.nuclphysb.2022.115675>.
 - [36] G. Branco, P. Ferreira, L. Lavoura, M. Rebelo, M. Sher, and J. P. Silva, *Physics Reports* **516**, 1 (2012), ISSN 0370-1573,

- theory and phenomenology of two-Higgs-doublet models, URL <https://www.sciencedirect.com/science/article/pii/S0370157312000695>.
- [37] L. Wang, J. M. Yang, and Y. Zhang, *Commun. Theor. Phys.* **74**, 097202 (2022), 2203.07244.
 - [38] S. P. Martin, *Adv. Ser. Direct. High Energy Phys.* **18**, 1 (1998), hep-ph/9709356.
 - [39] M. A. Luty, in *Theoretical Advanced Study Institute in Elementary Particle Physics: Physics in $D \geq 4$* (2005), pp. 495–582, hep-th/0509029.
 - [40] V. S. Mummidi, P. Lamba, and S. K. Vempati, *Indian J. Phys.* **97**, 3315 (2023), 2306.05797.
 - [41] T. D. Lee, *Phys. Rev. D* **8**, 1226 (1973).
 - [42] A. I. Bochkarev, S. V. Kuzmin, and M. E. Shaposhnikov, *Phys. Lett. B* **244**, 275 (1990).
 - [43] N. Turok and J. Zadrozny, *Nucl. Phys. B* **358**, 471 (1991).
 - [44] J. M. Cline and P.-A. Lemieux, *Phys. Rev. D* **55**, 3873 (1997), hep-ph/9609240.
 - [45] L. Fromme, S. J. Huber, and M. Seniuch, *JHEP* **11**, 038 (2006), hep-ph/0605242.
 - [46] J. M. Cline, K. Kainulainen, and M. Trott, *Journal of High Energy Physics* **2011** (2011), ISSN 1029-8479, URL [http://dx.doi.org/10.1007/JHEP11\(2011\)089](http://dx.doi.org/10.1007/JHEP11(2011)089).
 - [47] G. C. Dorsch, S. J. Huber, and J. M. No, *JHEP* **10**, 029 (2013), 1305.6610.
 - [48] B. Abi, T. Albahri, S. Al-Kilani, D. Allspach, L. Alonzi, A. Anastasi, A. Anisenkov, F. Azfar, K. Badgley, S. Baeßler, et al., *Physical Review Letters* **126** (2021), ISSN 1079-7114, URL <http://dx.doi.org/10.1103/PhysRevLett.126.141801>.
 - [49] S. W. Allen, A. E. Evrard, and A. B. Mantz, *Ann. Rev. Astron. Astrophys.* **49**, 409 (2011), 1103.4829.
 - [50] C. L. Sarazin, *X-ray emission from clusters of galaxies* (1988).
 - [51] S. W. Allen, D. A. Rapetti, R. W. Schmidt, H. Ebeling, R. G. Morris, and A. C. Fabian, *Monthly Notices of the Royal Astronomical Society* **383**, 879 (2008), ISSN 0035-8711, <https://academic.oup.com/mnras/article-pdf/383/3/879/3466307/mnras0383-0879.pdf>, URL <https://doi.org/10.1111/j.1365-2966.2007.12610.x>.
 - [52] Ettori, S., Morandi, A., Tozzi, P., Balestra, I., Borgani, S., Rosati, P., Lovisari, L., and Terenziani, F., *A&A* **501**, 61 (2009), URL <https://doi.org/10.1051/0004-6361/200810878>.
 - [53] A. B. Mantz, S. W. Allen, R. G. Morris, D. A. Rapetti, D. E. Applegate, P. L. Kelly, A. von der Linden, and R. W. Schmidt, *Monthly Notices of the Royal Astronomical Society* **440**, 2077 (2014), ISSN 0035-8711, <https://academic.oup.com/mnras/article-pdf/440/3/2077/23991383/stu368.pdf>, URL <https://doi.org/10.1093/mnras/stu368>.
 - [54] I. Mendonça, K. Bora, R. Holanda, S. Desai, and S. Pereira, *Journal of Cosmology and Astroparticle Physics* **2021**, 034 (2021), ISSN 1475-7516, URL <http://dx.doi.org/10.1088/1475-7516/2021/11/034>.
 - [55] I. Mendonça, K. Bora, R. Holanda, and S. Desai, *Journal of Cosmology and Astroparticle Physics* **2021**, 084 (2021), ISSN 1475-7516, URL <http://dx.doi.org/10.1088/1475-7516/2021/10/084>.
 - [56] R. F. L. Holanda, S. H. Pereira, V. C. Busti, and C. H. G. Bessa, *Classical and Quantum Gravity* **34**, 195003 (2017), 1705.05439.
 - [57] R. F. L. Holanda, S. H. Pereira, and S. Santos da Costa, *Phys. Rev. D* **95**, 084006 (2017), 1612.09365.
 - [58] S. Sasaki, *Publications of the Astronomical Society of Japan* **48**, L119–L122 (1996), ISSN 2053-051X, URL <http://dx.doi.org/10.1093/pasj/48.6.L119>.
 - [59] M. A. Dopita and R. S. Sutherland, *Astrophysics of the Diffuse Universe*, Astronomy and Astrophysics Library (Springer Berlin, Heidelberg, 2003).
 - [60] P. J. E. Peebles, *Principles of Physical Cosmology* (1993).
 - [61] F. M. White, *Fluid Mechanics* (McGraw-Hill, 2011), 7th ed.
 - [62] S. Planelles, S. Borgani, K. Dolag, S. Ettori, D. Fabjan, G. Murante, and L. Tornatore, *Monthly Notices of the Royal Astronomical Society* **431**, 1487 (2013), ISSN 0035-8711, <https://academic.oup.com/mnras/article-pdf/431/2/1487/4265857/stt265.pdf>, URL <https://doi.org/10.1093/mnras/stt265>.
 - [63] A. B. Mantz, R. G. Morris, S. W. Allen, R. E. A. Canning, L. Baumont, B. Benson, L. E. Bleem, S. R. Ehlert, B. Floyd, R. Herbonnet, et al., *Monthly Notices of the Royal Astronomical Society* **510**, 131–145 (2021), ISSN 1365-2966, URL <http://dx.doi.org/10.1093/mnras/stab3390>.
 - [64] D. E. Applegate, A. von der Linden, P. L. Kelly, M. T. Allen, S. W. Allen, P. R. Burchat, D. L. Burke, H. Ebeling, A. Mantz, and R. G. Morris, *Monthly Notices of the Royal Astronomical Society* **439**, 48 (2014), ISSN 0035-8711, <https://academic.oup.com/mnras/article-pdf/439/1/48/5560953/stt2129.pdf>, URL <https://doi.org/10.1093/mnras/stt2129>.
 - [65] D. E. Applegate, A. Mantz, S. W. Allen, A. von der Linden, R. G. Morris, S. Hilbert, P. L. Kelly, D. L. Burke, H. Ebeling, D. A. Rapetti, et al., *Mon. Not. R. Astron. Soc.* **457**, 1522 (2016), 1509.02162.
 - [66] Planck Collaboration, N. Aghanim, Y. Akrami, M. Ashdown, J. Aumont, C. Baccigalupi, M. Ballardini, A. J. Banday, R. B. Barreiro, N. Bartolo, et al., *Astron. & Astrophys.* **641**, A6 (2020), 1807.06209.
 - [67] D. M. Scolnic, D. O. Jones, A. Rest, Y. C. Pan, R. Chornock, R. J. Foley, M. E. Huber, R. Kessler, G. Narayan, A. G. Riess, et al., *The Astrophysical Journal* **859**, 101 (2018), ISSN 1538-4357, URL <http://dx.doi.org/10.3847/1538-4357/aab9bb>.
 - [68] Y. B. Zeldovich, I. Y. Kobzarev, and L. B. Okun, *Zh. Eksp. Teor. Fiz.* **67**, 3 (1974).
 - [69] T. Melo (2020), URL <https://repositorio.ufpb.br/jspui/handle/123456789/19693>.
 - [70] E. A. Paschos, *Phys. Rev. D* **15**, 1966 (1977), URL <https://link.aps.org/doi/10.1103/PhysRevD.15.1966>.
 - [71] S. L. Glashow and S. Weinberg, *Phys. Rev. D* **15**, 1958 (1977), URL <https://link.aps.org/doi/10.1103/PhysRevD.15.1958>.
 - [72] W. Ubachs, J. Bagdonaite, E. J. Salumbides, M. T. Murphy, and L. Kaper, *Rev. Mod. Phys.* **88**, 021003 (2016), URL <https://link.aps.org/doi/10.1103/RevModPhys.88.021003>.

- [73] J. D. Barrow and J. a. Magueijo, Phys. Rev. D **72**, 043521 (2005), URL <https://link.aps.org/doi/10.1103/PhysRevD.72.043521>.
- [74] M. Seikel and C. Clarkson, arXiv preprint arXiv:1311.6678 (2013).
- [75] s.-l. d. B. L. Copyright 2007 2024, *Rbf kernel documentation*, https://scikit-learn.org/stable/modules/generated/sklearn.gaussian_process.kernels.RBF.html [Accessed: (22/12/2024)].
- [76] F. Pedregosa, G. Varoquaux, A. Gramfort, V. Michel, B. Thirion, O. Grisel, M. Blondel, P. Prettenhofer, R. Weiss, V. Dubourg, et al., the Journal of machine Learning research **12**, 2825 (2011).
- [77] F. J. Botella, F. Cornet-Gomez, C. Miró, and M. Nebot, The European Physical Journal C **82** (2022), ISSN 1434-6052, URL <http://dx.doi.org/10.1140/epjc/s10052-022-10893-x>.
- [78] J. Kim, Physics Letters B **832**, 137220 (2022), ISSN 0370-2693, URL <https://www.sciencedirect.com/science/article/pii/S0370269322003549>.
- [79] T. Aaltonen et al. (CDF), Science **376**, 170 (2022).